Quantitative analysis of magnon characteristics with unidirectional magnetoresistance

Nyun Jong Lee[1,‡], Heechan Jang,[1,2,‡] Eunkang Park,[1] Ki-Seung Lee,[3] Seyeop Jeong,[1]
Soogil Lee,[4,5] Byong-Guk Park,[4] Chun-Yeol You,[3] Kyoung-Whan Kim,[6,*] and Sanghoon Kim[1,†]

[1]*Department of Physics and Energy Harvest Storage Research Center, University of Ulsan, Ulsan 44610,
Republic of Korea*

[2]*Institute for Chemical Research, Kyoto University, Uji, Kyoto, 611-0011, Japan*

[3]*Department of Emerging Materials Science, Daegu Gyeongbuk Institute of Science & Technology, Daegu 42988,
Republic of Korea*

[4]*Department of Materials Science and Engineering, Korea Advanced Institute of Science and Technology,
Daejeon 34141, Republic of Korea*

[5]*Department of Electronic Engineering, Gachon University, Seongnam 13120, Republic of Korea*

[6]*Center for Spintronics, Korea Institute of Science and Technology, Seoul 02792, Republic of Korea*

Unidirectional magnetoresistance (UMR) is a magnetoresistance family that arises from spin-current generation in ferromagnet (FM)/nonmagnetic heavy metal (HM) bilayers. Because UMR exhibits asymmetric behavior owing to the current or external magnetic field directions, it is easy to quantify the amount of charge-to-spin conversion in a system and the sign of the spin current. UMR has been explained by two major mechanisms: spin accumulation at the FM/HM interface and electron-magnon scattering in an FM layer. In this study, we investigated the thickness and temperature dependence of the UMR of Ta/Co and Pt/Co bilayer structures and numerically analyzed the contribution of the electron-magnon scattering using a self-developed quantitative-analysis model. The magnon UMR was dominant in the Pt/Co samples, and the spin-accumulation-UMR and magnon-UMR trends were separated in the Ta/Co samples by thickness. The magnitude of the UMR strongly depends on the choice of the HM. Our findings provide a method to quantitatively separate the contributions of each mechanism.

I. INTRODUCTION

Unidirectional magnetoresistance (UMR) is a magnetoresistance family arising from spin-current generation in ferromagnet (FM)/nonmagnetic heavy metal (HM) bilayers under in-plane magnetization [1–6]. UMR exhibits asymmetric behavior owing to reversal of the current or external-magnetic-field direction, unlike other magnetoresistances, such as giant magnetoresistance (GMR) [7,8] and spin Hall magnetoresistance (SMR) [9]. That is, the resistance of an FM/HM bilayer depends on the relative direction between magnetization of the FM and spin polarization of the spin current induced by the spin Hall effect [10,11]. In addition, resistance, which depends on the current amplitude, contributes to the nonlinear properties of the UMR. UMR was first explained by the spin-accumulation mechanism [1,2], and electron-magnon

scattering has been proposed as another mechanism to explain UMR [3,4].

The two mechanisms are detailed as follows. The spin-accumulation mechanism explains the UMR as a result of the interfacial spin chemical potential induced by the spin Hall effect in the HM layer [1,2,6]. Avci *et al.* [1] suggested current-in-plane GMR as the main mechanism of the UMR, and Zhang and Vignale [2] provided an analytic theory of UMR based on a drift-diffusion model. According to Zhang and Vignale's theory, when the electric field is applied in the positive x direction (E_x), the magnitude of the UMR is given by

$$\Delta R/R = 6 \left(\frac{\sigma_{0,\text{F}} \lambda_{\text{FM}}}{\sigma_{0,\text{H}} t_{\text{HM}} + \sigma_{0,\text{F}} t_{\text{FM}}} \right)$$
$$\times \frac{(p_\sigma - p_N) \left(\frac{\theta_{\text{H}} E_x \lambda_{\text{HM}}}{\epsilon_{\text{F}}} \right) \tanh \left(\frac{t_{\text{HM}}}{2\lambda_{\text{HM}}} \right) \tanh \left(\frac{t_{\text{FM}}}{\lambda_{\text{FM}}} \right)}{1 + (1 - p_\sigma^2) \left(\frac{\sigma_{0,\text{F}} \lambda_{\text{HM}}}{\sigma_{0,\text{H}} \lambda_{\text{FM}}} \right) \tanh \left(\frac{t_{\text{FM}}}{\lambda_{\text{FM}}} \right) \coth \left(\frac{t_{\text{HM}}}{\lambda_{\text{HM}}} \right)}, \quad (1)$$

where $\sigma_{0,\text{H}}$ ($\sigma_{0,\text{F}}$), λ_{HM} (λ_{FM}), and t_{HM} (t_{FM}) are the bulk conductivity, spin diffusion length, and thickness of the

*kwk@kist.re.kr

†sanghoon.kim@ulsan.ac.kr

‡N.J.L. and H.J. contributed equally to this work.

HM (FM) layer, respectively. The subscripts "H" and "F" refer to the HM and the FM, respectively. p_σ is the spin polarization of conductivity, p_N is that of the density of states at the Fermi level (ϵ_F) of the FM, and θ_H is the bulk spin Hall angle of the HM layer [2]. According to Ref. [2], the factor $p_\sigma - p_N$ in Eq. (1) is proportional to the difference in the mobilities of the majority and minority electrons, so the sign of the UMR is determined by the relative direction of the higher-mobility spins and the interfacial spin accumulation, as one can speculate intuitively.

In the electron-magnon-scattering mechanism, UMR is caused by high-energy magnon excitations in the terahertz frequency range through a spin-flip process [3]. Following the spin-flip process, the magnon population is enhanced (or suppressed) when the spin injected from the HM to the FM is antiparallel (or parallel) to the magnetization of the FM layer [12]. A distinctive feature of this magnon UMR is that its magnitude decreases with temperature (T). This trend is different from the spin-transport characteristics observed in the conventional SMR [3,13], but this magnon effect can be understood from the decrease in the magnon diffusion length at lower T [14,15].

As mentioned above, spin accumulation and electron–magnon scattering are considerable mechanisms of UMR. However, the contribution of magnons to the UMR in the HM/FM system and its quantitative analysis are still questionable. In this study, we observed the dependence of UMR on the thickness and temperature in Ta/Co and Pt/Co bilayer structures and analyzed the trend using an analysis model involving the magnon contribution. Three notable results were obtained from the analysis: (1) the UMR for both systems strongly depends on T and the thickness; (2) the magnon contribution is clearly distinguished from the spin accumulation in the Ta/Co systems, whereas the UMR of the Pt/Co systems was elucidated mainly by our model; and (3) the magnon contribution was successfully quantified with our model. Our study elucidates the effect of magnon generation on the spin transport in the system.

II. RESULTS

Figure 1(a) shows the sample structures of the HM (4 nm)/Co (t_{FM}) bilayer system deposited by the sputtering technique. Ta and Pt with different spin Hall angles were chosen as the HM [16,17]. The thickness of the Co layer (t_{FM}) ranged from 2 to 10 nm. A 2 nm-thick SiO_2 layer was used as the capping layer to prevent oxidation of Co. The measurement geometry is illustrated in Fig. 1(b). A triple Hall bar with width (w) of 10 μm and length (L) of 35 μm was patterned via photolithography.

The transport measurements were performed at various temperatures in a cryogen-free measurement system (Cryogenic Ltd.) with use of a standard lock-in technique

(NF Corp. LI5650) by application of an alternating current (I_{ac}) along the x direction with frequency $f = 17$ Hz (Keithley 6221). The second-harmonic magnetoresistance was acquired by our measuring the first and second harmonics of the longitudinal resistance (R_ω and $R_{2\omega}$) with a sweeping magnetic field (H) and dividing $R_{2\omega}$ into the first-harmonic resistance R_ω at zero magnetic field (denoted by R), as shown in Figs. 1(c) and 1(d). The two spikes shown in the inset in Fig. 1(d) are attributed to the low-energy magnons (gigahertz regime), because of the perpendicular anisotropy at the Pt/Co interface acting as a demagnetizing field [1]. The difference in resistance ($\Delta R_{2\omega}$) was obtained from half of the $R_{2\omega}$ change as a function of H. The opposite signs of $\Delta R_{2\omega}$ are due to the spin Hall angles of Ta and Pt. $\Delta R_{2\omega}$ includes an inevitable thermoelectric contribution ($\Delta R_{2\omega}^{\nabla T}$) from the anomalous Nernst effect. $\Delta R_{2\omega}^{\nabla T}$ was evaluated with the method described in Ref. [18]. $\Delta R_{2\omega}^{\nabla T}$ for the Ta/Co series was larger than that for the Pt/Co series, as previously reported [1]. The pure UMR contribution $\Delta R_{2\omega}^{UMR}$ was acquired by our subtracting $\Delta R_{2\omega}^{\nabla T}$ evaluated with the method suggested in Ref. [18]; $\Delta R_{2\omega}^{UMR} = \Delta R_{2\omega}^{total} - R_{2\omega}^{\nabla T}$. The detailed process for subtraction of the thermoelectric effect is described in Supplemental Material [19].

UMR is strongly related to the current density of each layer and the spin current generated in the HM layer. The current density of each layer was varied in these metallic bilayer systems owing to the shunting effect. To evaluate the current density in the HM layer (J_{HM}), the thickness of each layer was determined with a vibrating-sample magnetometer and x-ray-reflectometry measurements. On the basis of the results, the resistivity of each layer was obtained by our applying the surface-scattering-resistance [20] and parallel-resistance models (see Supplemental Material [19]). Figures 1(e) and 1(f) show the J_{HM}-dependent $\Delta R_{2\omega}^{UMR}$ at room temperature. $\Delta R_{2\omega}^{UMR}$ was linearly proportional to J_{HM} within the range of experimental conditions. The magnon contribution to the UMR was examined with respect to the normalized $\Delta R_{2\omega}^{UMR}$ acquired from the slope of $\Delta R_{2\omega}^{UMR} R^{-1}$ versus J_{HM}.

III. MAGNON-BASED TWO-CURRENT ANALYSIS MODEL FOR USMR

The normalized $\Delta R_{2\omega}^{UMR}$ is plotted as a function of t_{FM} in Fig. 2(a). The upper panel shows Ta/Co and the lower panel shows Pt/Co. For Ta/Co, the trend in the normalized $\Delta R_{2\omega}^{UMR}$ for $t_{FM} > 5$ nm does not follow the model predicted by Eq. (1) (dashed line). To analyze this trend, we proposed an analysis model based on the parallel-circuit model, which assumes two current paths in the FM layer, as illustrated in Fig. 2(b). In this model, one path is part of the magnon generation, and the other is an inactive part. The spin Hall current generated in the HM layer primarily excites the spin-flip magnons near the interfacial
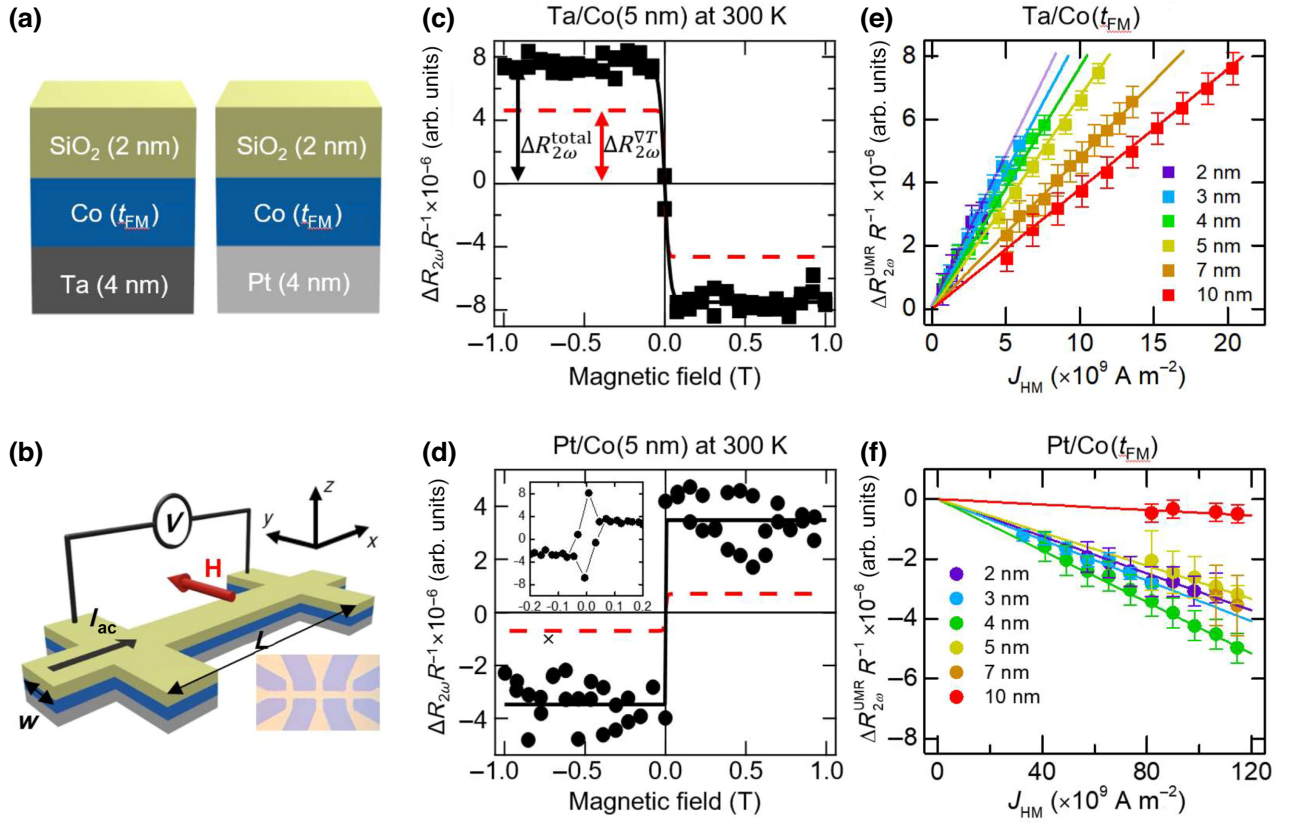
FIG. 1. (a) HM(4 nm)/Co(t_{FM})/SiO$_2$(2 nm) system and (b) UMR measurement geometry. The directions of I_{ac} and **H** correspond to the x and y directions, respectively. The inset shows an optical-microscopy image of a Hall-bar device. Normalized second-harmonic magnetoresistance, $\Delta R_{2\omega}^{UMR} R^{-1}$ of (c) Ta/Co(5 nm) and (d) Pt/Co(5 nm) as a function of magnetic field **H** at 300 K with current densities $J_{HM} = 2.03 \times 10^{10}$ A/m^2 for Ta/Co and $J_{HM} = 11.0 \times 10^{10}$ A/m^2 for Pt/Co, respectively. Dashed red lines indicate $\Delta R_{2\omega}^{\nabla T}$ from the anomalous Nernst effect. Variation of $\Delta R_{2\omega}^{UMR}$ as a function of J_{HM} for (e) Ta/Co(t_{FM}) and (f) Pt/Co(t_{FM}). Solid lines are linear fits of the data. Different colors correspond to the different thicknesses, which are denoted in the legend.

region once they have been injected into the FM layer. The magnon propagates into the FM bulk part with a finite decay length, which is defined as the magnon diffusion length. We suspect that the primary origin of magnon diffusion is electron-magnon scattering; however, its exact origin does not affect our analysis. In reality, although the "activity" of the magnon excitation decayed continuously as the magnon propagated deeper and deeper, we modeled this behavior as a simple step function so that the magnons were excited within depth t_0 (called "active region") while the magnon generation was completely suppressed in the deeper region (called "inactive region"). Therefore, the thickness of the active region (t_0) corresponds to the incoherent magnon diffusion length or quantum-spin-flip range in practice. This simplification allowed us to model the experimental data using a simple two-current model.

Because magnons are generated with injected spins that are antiparallel to the localized spins in the FM layer, the magnetoresistance can be defined as $\Delta R/R =$

$(R_{\uparrow\downarrow} - R_{\uparrow\uparrow})/R_{\uparrow\uparrow}$, where $R_{\uparrow\downarrow}$ and $R_{\uparrow\uparrow}$ are the resistances when the accumulated spin and magnetization of the FM are antiparallel and parallel, respectively. Assuming a parallel circuit, these resistances can be defined as

$$R_{\uparrow\downarrow} = \frac{(R_0 + \Delta R_{magnon})R_1}{R_0 + \Delta R_{magnon} + R_1}, \quad R_{\uparrow\uparrow} = \frac{R_0 R_1}{R_0 + R_1}, \quad (2)$$

where R_0 is the resistance of the active layer, R_1 is the resistance of the inactive layer, and ΔR_{magnon} is the increase in resistance owing to electron-magnon scattering. Therefore, two current paths can be considered: one where the resistance increases owing to magnon generation and one that is unrelated to the magnon-based magnetoresistance. When interfacial spins are parallel to the magnetization of the FM layer, the entire FM layer is inactive. As the spin-flip process occurs, the active layer becomes thicker, leading to a change in the resistance.
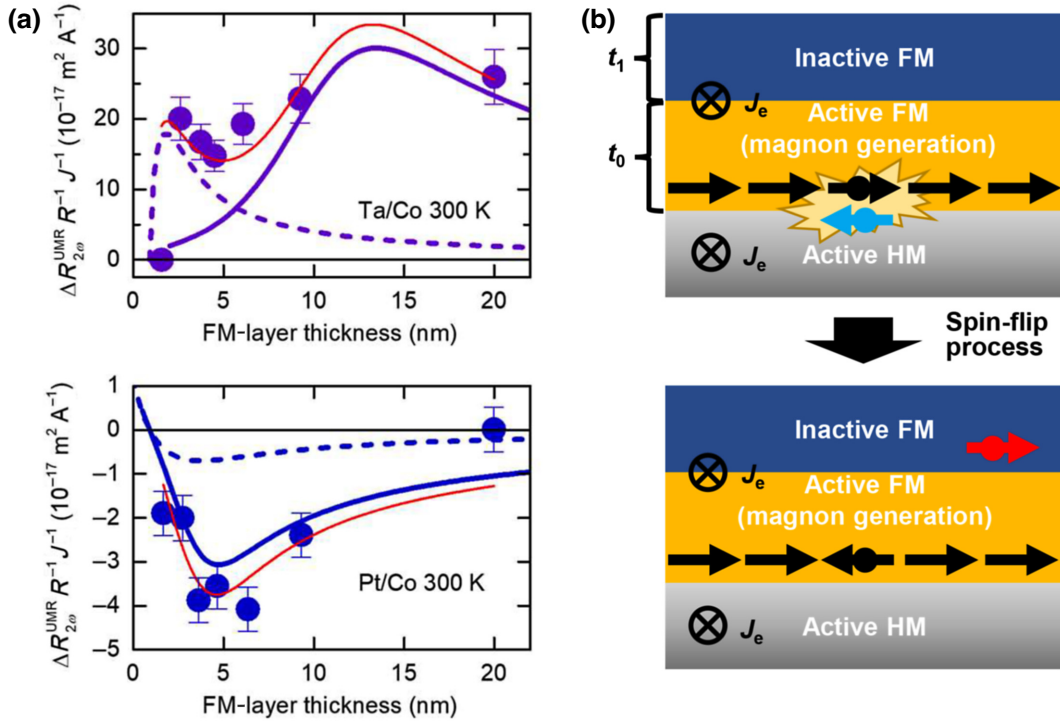
FIG. 2. (a) t_{FM} dependence of UMR at room temperature ($T = 300$ K). The normalized $\Delta R_{2\omega}^{UMR}$ for the Ta/Co series (purple) and that for the Pt/Co series (blue) are fitted to a linear combination (red line) of the magnon two-current UMR model (solid line) and spin-accumulation model (dashed line). For the Ta/Co series, the spin-accumulation UMR shows a dominant contribution for small thickness, whereas the magnon UMR dominantly contributes for large thickness. For the Pt/Co series (blue), the normalized $\Delta R_{2\omega}^{UMR}$ is fitted to the magnon two-current UMR dominantly. (b) Magnon two-current UMR model. In an active FM layer (yellow layer), a magnon is generated through a spin-flip process when the spin from the HM layer has antiparallel alignment with the localized spin in the FM layer, and the diffused magnon gives rise to electron-magnon scattering.

From Eq. (2), the UMR is given by

$$\left(\frac{\Delta R}{R}\right) = \left(\frac{\Delta R_{magnon}}{R_0}\right) \frac{R_1}{R_1 + R_0}$$

$$= \left(\frac{\Delta R_{magnon}}{R_0}\right) \frac{G_{HM} + t_0 w/L\rho_{FM}^{-1}}{G_{HM} + t_{FM} w/L\rho_{FM}^{-1}}, \quad (3)$$

where w and L are the width and length of a current path, respectively. The scattering events included the spin-dependent scattering contribution in the FM layer of $1 - \exp(-t_{FM}/t_0)$, the spin-diffusion scattering contribution in the FM, and interfacial spin conductance [21–23]. Then UMR is finally obtained as follows:

$$\left(\frac{\Delta R_{2\omega}}{R_0}\right) = \frac{2A_0}{B + \coth\left(\frac{t_{FM}}{2t_0}\right)} \frac{1}{1 + \frac{t_{FM} w}{L G_{HM} \rho_{FM}}}, \quad (4)$$

where G_{HM} is the conductance of the HM layer and ρ_{FM} is the resistivity of the FM layer. A_0 refers to the FM-independent amplitude of the UMR, which is generally a function of the thickness and spin diffusion length of the HM layer. This model has the same form as the

two-current model of the GMR effect, considering both the interface and bulk effects suggested by Dieny *et al.* [21]. From this approach, we obtained $B = 1$, but when we consider a more-complicated model without assuming the active region, B may deviate from 1 in a diffusion formalism (see Supplemental Material [19] for the derivation). As shown in Fig. 2(a), the linear combination of the spin-accumulation model and our magnon-based model successfully reproduced the trend of the normalized $\Delta R_{2\omega}^{UMR}$ for Ta/Co and Pt/Co (see Supplemental Material [19] for the fitting procedure). Thus, the magnon and spin-accumulation contributions can be separated and the different behaviors under various conditions can be observed.

Thus, we investigated the T-dependent normalized $\Delta R_{2\omega}^{UMR}$ in terms of t_{FM} and showed that the qualitative behaviors of the two contributions were completely different. Figures 3(a) and 3(b) show the t_{FM} dependence of the normalized $\Delta R_{2\omega}^{UMR}$ at various T values for Ta/Co [Fig. 3(a)] and Pt/Co [Fig. 3(b)]. In both cases, the UMR for $t_{FM} > 5$ nm is fully suppressed as T decreases. This suppression is reasonable considering the decrease in the magnon diffusion length at lower T [14,15]. The trends for
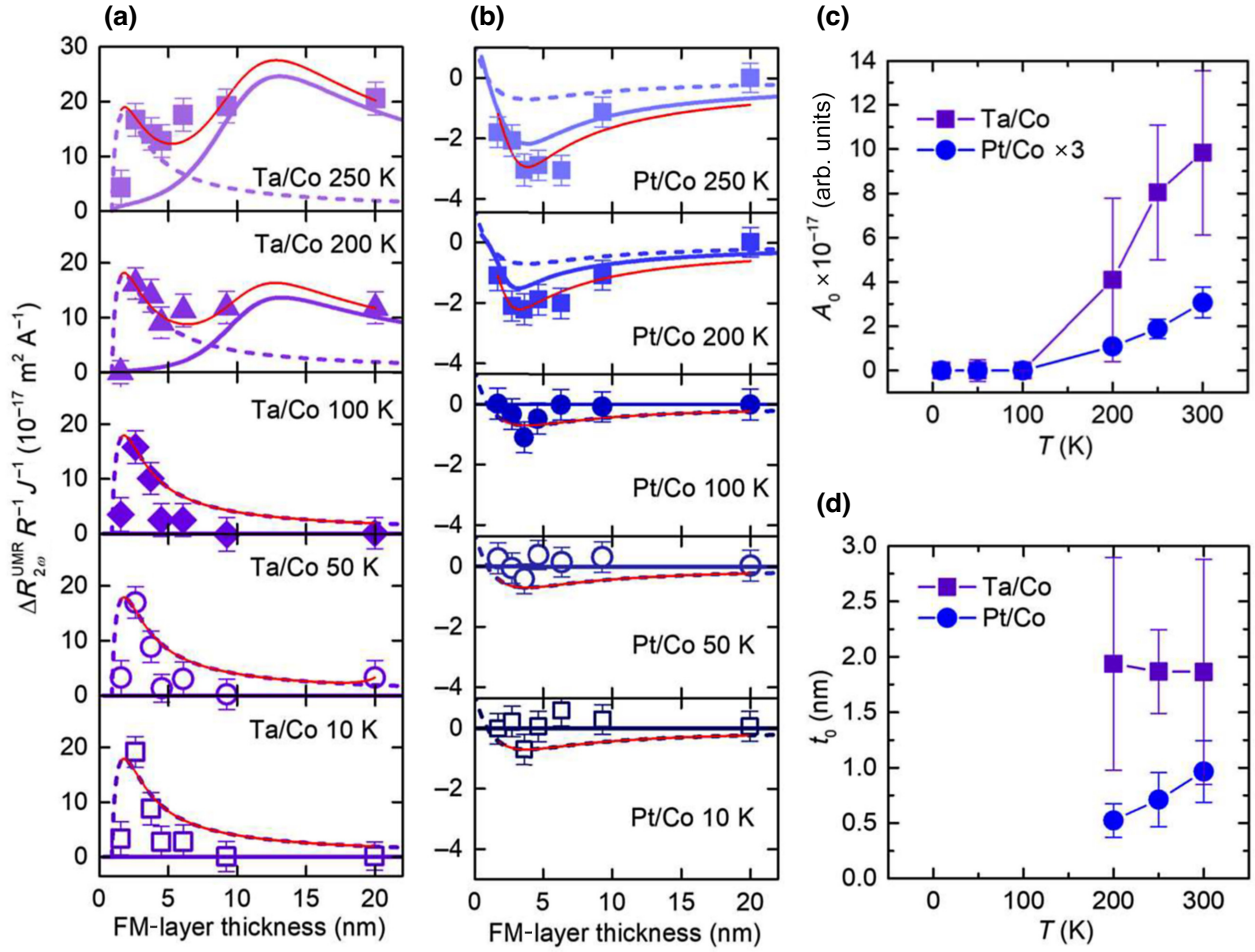
FIG. 3. T and t_{FM} dependence of UMR in (a) Ta/Co and (b) Pt/Co systems. Different symbols correspond to the different temperatures denoted in the legend. Solid and dashed lines denote fits to the UMR according to the suggested magnon UMR model (solid line) and the spin-accumulation model (dashed line). (c),(d) Comparison of fitting parameters A_0 and t_0 as a function of T.

both cases followed the magnon-based model suggested in this study [solid line in Figs. 3(a) and 3(b)]. However, the Ta/Co series shows T independence in the range of $t_{FM} \leq 5$ nm, which follows the spin-accumulation picture as a dotted line in Fig. 3(a) [Eq. (1)]. The observed UMRs clearly showed distinct trends between magnon-based and spin-accumulation-based UMRs as a function of T.

IV. DISCUSSION

Our findings suggest that two models are required to explain the observed UMR, particularly for the Ta/Co series. On the basis of the best fit of Eq. (4), we obtained A_0 and t_0 as functions of T, as shown in Figs. 3(c) and 3(d), where A_0 and t_0 correspond to the UMR amplitude and magnon diffusion length, respectively. A_0 decreases with T from 300 to 100 K, and it becomes zero below 100 K; t_0 shows a similar trend to that of A_0, a counterdependence of T compared with the spin-flip diffusion length of Co [24].

Here we stress that different characteristic lengths between spin accumulation and magnon generation are observed in Ta/Co, whereas in Pt/Co they are almost the same. When $T > 100$ K, t_0 in Ta/Co is greater than in Pt/Co, $t_0 \sim 2$ nm for Ta/Co and $t_0 \sim 0.5$–1.0 nm for Pt/Co. This is consistent with the fact that the Pt/Co interface has a larger damping than the Ta/Co interface [25], and thus it exhibits a shorter magnon diffusion length. This explains why more magnons can diffuse in Ta/Co, and as a result, A_0 of Ta/Co is larger than that of Pt/Co. We also need to consider that a higher spin Hall angle should lead to a higher magnon population. β-Ta is known to have a larger spin Hall angle (approximately 0.3) than Pt (approximately 0.1–0.2) [26]. Another point we found in this observation is that the evaluated magnon diffusion length t_0 is much less than other reported values [27]. Such small t_0 is attributed to the frequency (ω) and coherency. The excited magnons in this measurement are incoherent with the terahertz range [28]. In general, the magnon

$$\frac{1}{B + \coth\frac{t_{FM}}{2t_0}}$$

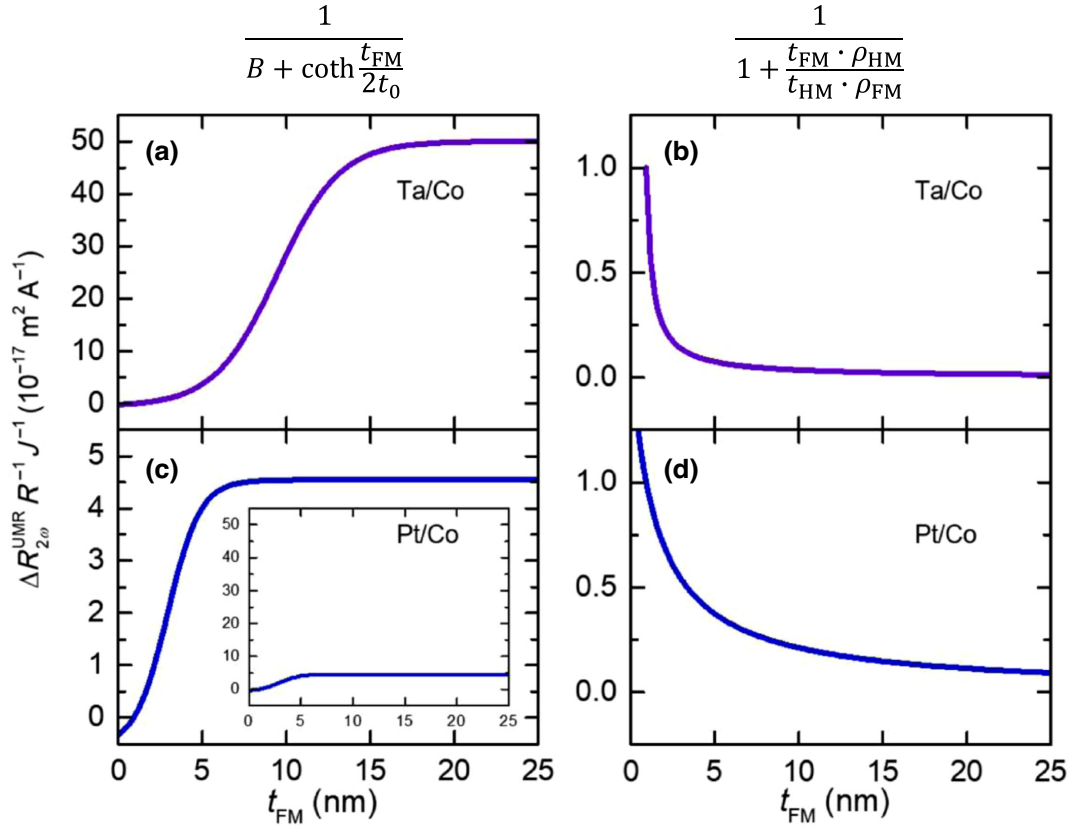$$\frac{1}{1 + \frac{t_{FM} \cdot \rho_{HM}}{t_{HM} \cdot \rho_{FM}}}$$

FIG. 4. $1/\{B + \coth(t_{FM}/2t_0)\}$ contribution to the UMR in (a) Ta/Co and (b) Pt/Co systems as a function of t_{FM} and $1/\{1 + (t_{FM}\rho_{HM})/(t_{HM}\rho_{FM})\}$ contribution to the UMR in (c) Ta/Co and (d) Pt/Co systems as a function of t_{FM}. The inset in (c) presents the same data on a different scale to match that shown in (a).

decay length, $L_{decay} = v_g \tau_{mag}$, where v_g and τ_{mag} are the group velocity and magnon lifetime, respectively. Considering that $v_g \sim d\omega/dk$ and $\tau_{mag} \sim 1/\alpha\omega$, where k and α are the wave number and the damping constant, $L_{decay} \propto d\ln\omega/dk$. Qualitatively, these relations indicate that high ω decreases L_{decay}. These observations confirm that the procedure suggested here not only allows the separation of different mechanisms of UMR but is also useful for characterizing the generation of the incoherent terahertz magnon population and its transport in the FM.

To understand the physical meaning of the peak in the curve fitted with Eq. (4), we separately confirmed the t_{FM} dependence of terms $1/\{B + \coth(t_{FM}/2t_0)\}$ and

$1/\{1 + (t_{FM}\rho_{HM})/(t_{HM}\rho_{FM})\}$ as shown in Fig. 4. We note that the $1/\{B + \coth(t_{FM}/2t_0)\}$ term shows saturating behavior, which is related to the magnon diffusion length. On the other hand, the term $1/\{1 + (t_{FM}\rho_{HM})/(t_{HM}\rho_{FM})\}$, related to shunting current, decreases with t_{FM}. These two different contributions give rise to the peak in the fitted curve. We note that the contribution of $1/\{B + \coth(t_{FM}/2t_0)\}$ saturates when t_{FM} is about sevenfold and fourfold larger than t_0 in case of Ta/Co and Pt/Co, respectively. Therefore, t_{FM} should be sufficiently large to observe the UMR in a system.

V. CONCLUSION

In conclusion, we investigated the dependence of UMR on temperature and the thickness of the FM layer and developed a quantitative-analysis model for the magnon contribution of UMR in HM/FM bilayer structures. We established that magnon UMR is dominant in Pt/Co samples, and the spin-accumulation-UMR and magnon-UMR trends are separated in the Ta/Co samples by thickness. The magnon UMR can be quantified by the

TABLE I. Fitting parameters for Ta/Co and Pt/Co systems evaluated through the best fit of the magnon-based two-current model.

	t_{HM} (nm)	λ_{HM} (nm)	$t_{HM}\rho_{FM}/\rho_{HM}$ (nm)	B	t_{FM}/t_0 at maxima
Ta/Co	4.0	2.0	0.3	−0.98	∼6.8
Pt/Co	4.0	10.0	2.4	−0.78	∼3.9

active-layer thickness t_0, which is the characteristic thickness of magnon generation by the spin-flip process. Our results indicate that the magnon mechanism is significant in the HM/FM bilayer system. In addition, we suggest a possible analysis method that quantifies the incoherent terahertz magnon characteristics using only electrical measurements (Table I).

ACKNOWLEDGMENTS

[1] C. O. Avci, K. Garello, A. Ghosh, M. Gabureac, S. F. Alvarado, and P. Gambardella, Unidirectional spin Hall magnetoresistance in ferromagnet/normal metal bilayers, Nat. Phys. **11**, 570 (2015).

[2] S. S. L. Zhang and G. Vignale, Theory of unidirectional spin Hall magnetoresistance in heavy-metal/ferromagnetic-metal bilayers, Phys. Rev. B **94**, 140411(R) (2016).

[3] K.-J. Kim, T. Li, S. Kim, T. Moriyama, T. Koyama, D. Chiba, K.-J. Lee, H.-W. Lee, and T. Ono, Possible contribution of high energy magnons on the unidirectional magnetoresistance in metallic bilayers, Appl. Phys. Express **12**, 063001 (2019).

[4] K. Yasuda, A. Tsukazaki, R. Yoshimi, K. S. Takahashi, M. Kawasaki, and Y. Tokura, Large unidirectional magnetoresistance in a magnetic topological insulator, Phys. Rev. Lett. **117**, 127202 (2016).

[5] Y. Yin, D.-S. Han, M. C. H. de Jong, R. Lavrijsen, R. A. Duine, H. J. M. Swagten, and B. Koopmans, Thickness dependence of unidirectional spin-Hall magnetoresistance in metallic bilayers, Appl. Phys. Lett. **111**, 232405 (2017).

[6] C. O. Avci, J. Mendil, G. S. D. Beach, and P. Gambardella, Origins of the unidirectional spin Hall magnetoresistance in metallic bilayers, Phys. Rev. Lett. **121**, 087207 (2018).

[7] G. Binasch, P. Grünberg, F. Saurenbach, and W. Zinn, Enhanced magnetoresistance in layered magnetic structures with antiferromagnetic interlayer exchange, Phys. Rev. B **39**, 4828 (1989).

[8] M. N. Baibich, J. M. Broto, A. Fert, F. Nguyen Van Dau, F. Petroff, P. Etienne, G. Creuzet, A. Friederich, and J. Chazelas, Giant magnetoresistance of (001)Fe/(001)Cr magnetic superlattices, Phys. Rev. Lett. **61**, 2472 (1988).

[9] H. Nakayama, M. Althammer, Y.-T. Chen, K. Uchida, Y. Kajiwara, D. Kikuchi, T. Ohtani, S. Geprägs, M. Opel, S. Takahashi, R. Gross, G. E. W. Bauer, S. T. B. Goennenwein, and E. Saitoh, Spin Hall magnetoresistance induced by a nonequilibrium proximity effect, Phys. Rev. Lett. **110**, 206601 (2013).

[10] J. E. Hirsch, Spin Hall effect, Phys. Rev. Lett. **83**, 1834 (1999).

[11] J. Sinova, D. Culcer, Q. Niu, N. A. Sinitsyn, T. Jungwirth, and A. H. MacDonald, Universal intrinsic spin Hall effect, Phys. Rev. Lett. **92**, 126603 (2004).

[12] K.-J. Kim, T. Moriyama, T. Koyama, D. Chiba, S. W. Lee, S. J. Lee, K. J. Lee, H. W. Lee, and T. Ono, Current-induced asymmetric magnetoresistance due to energy transfer via quantum spin-flip process, preprint arXiv:1603.08746 (2016).

[13] J. Kim, P. Sheng, S. Takahashi, S. Mitani, and M. Hayashi, Spin Hall magnetoresistance in metallic bilayers, Phys. Rev. Lett. **116**, 097201 (2016).

[14] B. Raquet, M. Viret, E. Sondergard, O. Cespedes, and R. Mamy, Electron-magnon scattering and magnetic resistivity in 3d ferromagnets, Phys. Rev. B **66**, 024433 (2002).

[15] L. J. Cornelissen, J. Shan, and B. J. van Wees, Temperature dependence of the magnon spin diffusion length and magnon spin conductivity in the magnetic insulator yttrium iron garnet, Phys. Rev. B **94**, 180402(R) (2016).

[16] L. Liu, C.-F. Pai, Y. Li, H. W. Tseng, D. C. Ralph, and R. A. Buhrman, Spin-torque switching with the giant spin Hall effect of tantalum, Science **336**, 555 (2012).

[17] L. Liu, T. Moriyama, D. C. Ralph, and R. A. Buhrman, Spin-torque ferromagnetic resonance induced by the spin Hall effect, Phys. Rev. Lett. **106**, 036601 (2011).

[18] C. O. Avci, K. Garello, M. Gabureac, A. Ghosh, A. Fuhrer, S. F. Alvarado, and P. Gambardella, Interplay of spin-orbit torque and thermoelectric effects in ferromagnet/normal-metal bilayers, Phys. Rev. B **90**, 224427 (2014).

[19] See Supplemental Material at http://link.aps.org/supplemental/10.1103/PhysRevApplied.20.064006 for subtraction of the thermoelectric effect, measurement of the layer thickness for each film, estimation of the resistivities of Pt, Ta, and Co using the Fuch-Sondheimer surface-scattering model, the diffusion approach for Eq. (4), and the fitting procedure. References [1,20,29–32] are also cited in Supplemental Material.

[20] E. H. Sondheimer, The mean free path of electrons in metals, Adv. Phys. **50**, 499 (2001).

[21] B. Dieny, P. Humbert, V. S. Speriosu, S. Metin, B. A. Gurney, P. Baumgart, and H. Lefakis, Giant magnetoresistance of magnetically soft sandwiches: Dependence on temperature and on layer thicknesses, Phys. Rev. B **45**, 806 (1992).

[22] B. Dieny, V. S. Speriosu, and S. Metin, Thermal variation of the magnetoresistance of soft spin-valve multilayers, Europhys. Lett. **15**, 227 (1991).

[23] W. Zhang, M. B. Jungfleisch, W. Jiang, Y. Liu, J. E. Pearson, S. G. E. te Velthuis, A. Hoffmann, F. Freimuth, and

Y. Mokrousov, Reduced spin-Hall effects from magnetic proximity, Phys. Rev. B **91**, 115316 (2015).

[24] K. Gupta, R. J. H. Wesselink, Z. Yuan, and P. J. Kelly, Spin transport at finite temperature: A first-principles study for ferromagnetic|nonmagnetic interfaces, Phys. Rev. B **104**, 205426 (2021).

[25] X. Ma, G. Yu, C. Tang, X. Li, C. He, J. Shi, K. L. Wang, and X. Li, Interfacial Dzyaloshinskii-Moriya interaction: effect of 5*d* band filling and correlation with spin mixing conductance, Phys. Rev. Lett. **120**, 157204 (2018).

[26] X. Lin, W. Yang, K. L. Wang, and Z. Weisheng, Two-dimensional spintronics for low-power electronics, Nat. Electron. **2**, 274 (2019).

[27] A. Mahmoud, F. Ciubotaru, F. Vanderveken, A. V. Chumak, S. Hamdioui, C. Adelmann, and S. Cotofana, Introduction to spin wave computing, J. Appl. Phys. **128**, 161101 (2020).

[28] T. H. T. Nguyen, V. Q. Nguyen, S. Jeong, E. Park, H. Jang, N. J. Lee, S. Lee, B.-G. Park, S. Cho, H.-W. Lee, J.-I. Hong, and S. Kim, Unidirectional spin Hall magnetoresistance in epitaxial Cr/Fe bilayer from electron-magnon scattering, Commun. Phys. **4**, 247 (2021).

[29] H. S. Nalwa, *Handbook of Thin Film Materials* (Academic Press, San Diego, 2002), Vol. 5, Chapter 7 Magnetism of nanophase composite films, ISBN: 0-12-512913-0.

[30] S. R. Marmion, M. Ali, M. McLaren, D. A. Williams, and B. J. Hickey, Temperature dependence of spin Hall magnetoresistance in thin YIG/Pt films, Phys. Rev. B **89**, 220404 (2014).

[31] S. Meyer, M. Althammer, S. Geprägs, M. Opel, R. Gross, and S. T. B. Goennenwein, Temperature dependent spin transport properties of platinum inferred from spin Hall magnetoresistance measurements, Appl. Phys. Lett. **104**, 242411 (2014).

[32] M. Isasa, E. Villamor, L. E. Hueso, M. Gradhand, and F. Casanova, Temperature dependence of spin diffusion length and spin Hall angle in Au and Pt, Phys. Rev. B **91**, 024402 (2015).